

## CERAMIC-METAL COMPOSITES IN THE SYSTEM Ni-Al-O

S.M. Barinov, L.V. Fateeva, S.V. Yurashev, B. Ballóková, E. Rudnayová

### **Abstract**

*Ceramic-matrix alumina-(spinel)-nickel composites with superior mechanical properties were prepared using a chemical heterogeneous interaction method to synthesize the initial mixed hydroxide powders followed by the calcinations in air to convert the hydroxides into respective oxides, the partial reduction of metallic phase by hydrogen gas and the sintering in a vacuum or hot uniaxial pressing in an argon gas atmosphere. The effect of sintering activation additions of manganese and titanium oxides on the densification was studied. The features of the phase composition, microstructure and mechanical properties development in dependence on the fabrication route were investigated in detail.*

**Keywords:** *ceramic-metal composites, mechanical properties*

### **INTRODUCTION**

The strengthening and toughening of oxide ceramics by the incorporation of ductile metallic particulates have been studied extensively [1-8]. The effect is found to be dependent on the fabrication route and the microstructure formation features. The toughening is believed due to the bridging of ceramic grains by the metallic particulate. Therefore, the plastic deformation of the metal gives the main contribution to the dissipation of the loading work, and the state of the interfaces between the ceramic and metallic phases is the most important factor. The strength is primarily dependent on the grain size and residual stresses imposed upon constituents of the composite.

The composites can principally find application as a material for heat-resistant and thermal-shock-fracture resistant components in engines, and in cutting tools for metal working. Another prospective field of application is magnetic wear-resistant material, because the composites may reveal unusual magnetic behavior, e.g. high coercive force, if the magnetic particulate phase size is about a single domain dimension, the latter being of about 50 to 100 nm for nickel particles [2].

The main problems to fabricate such composites are the reduction of grain size and attaining of uniformity of the metallic and oxide constituents distribution in the sintered body. To solve these problems, chemical methods are applied to produce a large number of polyphase oxide-metal powders [9,10]. These methods provide potential advantages with respect to conventional processing techniques based on the mixing of metallic and oxide initial powders in ball mills or attritors. As an example, the nanostructured powders in the system Ni - ZrO<sub>2</sub> have been prepared by sol-gel chemical synthesis using zirconium propylate and nickel acetate as precursors [10]. It is known that the polymeric sol-gel route is the most successful technique to attain a good homogeneity on the atomic scale [11]. An alternative approach to the synthesis of multimetal cation oxides is a method of heterophase interaction [12]. The method is based on interaction of a particulate solid phase, e.g.

---

Sergej M. Barinov, Lydia V. Fateeva and Sergej V. Yurashev, Institute for Physical Chemistry of Ceramics RAS, Moscow, Russia

Beáta Ballóková, Emőke Rudnayová, Institute of Materials Research, Slovak Academy of Sciences, Košice, Slovak Republic

hydroxide comprising one type of metal ion, with a solution which contains the second metal cation. The release of protons by molecules of solid phase (hydroxide) and the addition of cations from the solution results in multimetal hydroxide having a stochastically-uniform distribution of the cations. By comparison with the polymeric sol-gel process, the heterophase interaction does easily allow a control of the characteristics of the product. This work is therefore aimed at the investigation of the chemical processing of the ultrafine powders in the system  $n\text{Al}_2\text{O}_3 \cdot m\text{NiO} - \text{Ni}$  by heterophase interaction followed by heat treatment and of the mechanical properties of sintered compacts.

## EXPERIMENTAL PROCEDURE

A method of heterophase interaction in aqueous solutions was utilized [8]. The starting components were  $\text{AlCl}_3 \cdot 6\text{H}_2\text{O}$ ,  $\text{NiCl}_2 \cdot 6\text{H}_2\text{O}$  and ammonia. The precipitation of  $\text{Al}(\text{OH})_3$  was performed by the treatment of  $\text{AlCl}_3 \cdot 6\text{H}_2\text{O}$  by 15M  $\text{NH}_4\text{OH}$  solution for 30 min. After washing and filtering, the precipitate was treated by 0.6M  $\text{NiCl}_2$  solution with an addition of 2.46M  $\text{NH}_4\text{OH}$  at pH 11. During a period of 60 min, the pH value was diminished to about 8. The precipitate was filtered and washed up to pH reaching 7, and then was dried at  $80^\circ\text{C}$ . The compositions were calculated to yield the precipitates of  $\text{Al}_x\text{Ni}_y(\text{OH})_z \cdot n\text{H}_2\text{O}$  hydroxides where x and y correspond to molar ratios of  $\text{Al}_2\text{O}_3/\text{NiO}$  to be equal to 70/30 (composition 1) and to 50/50 (composition 2). These ratios are in the two-phase  $\text{NiAl}_2\text{O}_4 - \text{Al}_2\text{O}_3$  and in the single-phase  $\text{NiAl}_2\text{O}_4$  regions of the equilibrium phase diagram, respectively. The subsolidus region of the nickel oxide - alumina phase equilibrium diagram is shown in Fig.1.

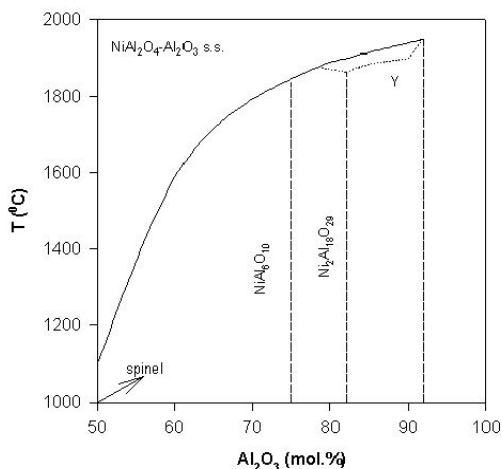


Fig.1. Subsolidus region of the phase equilibrium diagram  $\text{NiO} - \text{Al}_2\text{O}_3$  [13].

After that, the sintering additives of  $\text{TiO}_2$  or  $\text{MnO}$  in an amount of 0 to 2 wt.% were added to some green mixtures. The hydroxides with additives or without were further calcined in the air at a temperature of  $950^\circ\text{C}$  and above, in order to convert them into oxides. The oxide powders were characterised by BET specific area measurements by sorption-desorption isotherms of a purified nitrogen (a Quantachrome Autosorb), by X-ray diffractometry (XRD) and microscopic observations (a Neophote 32 microscope). The powder XRD method utilizing a DRON 3 diffractometer with  $\text{Cu K}_\alpha$  radiation ( $1.540598 \text{ \AA}$ ) was employed.

Afterwards, the oxide powders were treated in  $H_2$  at a temperature in the range 500 to 1000°C with the aim to reduce the NiO. Both the phase composition and the specific area were monitored by XRD and BET gas-adsorption measurements, respectively. Some experiments were performed with sintering to evaluate the mechanical properties of the compact composite bodies. The powders were subjected to: a) cold uniaxial pressing followed by sintering at a temperature 1520°C in a vacuum or b) hot uniaxial pressing at a temperature 1410°C and a pressure of 30 MPa during 15 minutes. The microstructure was studied with a Neophote-32 microscope and a Tesla scanning electron microscope equipped with an energy-dispersive X-ray microprobe. The three-point bending strength and fracture toughness (a single-edge notched beam technique [14]) of the specimens were measured using common techniques. The specimens for ultimate bending strength measurements were  $3 \times 5 \times 18 \text{ mm}^3$  in size. The tests were performed in a rigid three-point adjustment at a span of 12 mm using a UTS-100 testing machine. The cross-head velocity was  $1.7E-7 \text{ ms}^{-1}$ .

## RESULTS AND DISCUSSION

### Hydroxides

The yield of the precipitation products was 99.0-99.8 wt.%. XRD revealed that the precipitates are in an amorphous state. The size of the agglomerates was in the range from less than 1  $\mu\text{m}$  up to 50  $\mu\text{m}$ , as measured by an immersion-liquid optical microscopy method. The refraction indices  $n_g$  were equal to 1.560 and 1.565 for the compositions 1 and 2, respectively. DTA in the range from 20 to 1000°C showed two endothermal effects in the low-temperature range, as well as an exothermic effect at 800 to 1000°C, the latter being correspondent to crystallisation of the spinel-base solid solutions. This is confirmed by XRD measurements.

### Oxides

Figure 2 shows the dependence of BET specific area on calcination temperature. The specific area of the series 1 is higher than that for the series 2 powders. Specific area decreases monotonously with an increase of calcination temperature, probably due to the agglomeration of the powders, the effect being most pronounced for composition 1.

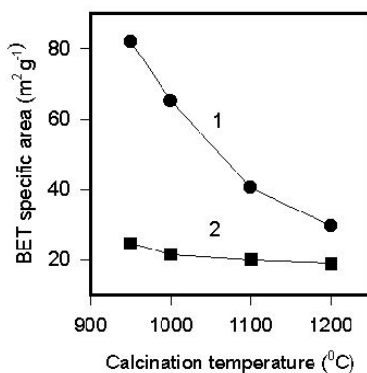


Fig.2. Effect of calcinations temperature on specific area of oxides of compositions 1 and 2.

The powders calcinated at 950°C were studied by XRD. It was particularly shown that the degree of crystallization is about 46% for composition 1, and ca. 70% for

composition 2, the samples of which were calcinated at 950°C. The products of crystallization were spinel-base solid solutions and spinel which contained small amounts of NiO for the series 1 and 2 of the samples, respectively. The phase composition is dependent upon calcination temperature. Heat-treated at 1200°C, the powders of composition 1 contain additionally small amounts of alpha-alumina crystals.

### Oxide-metal composite powders

Metallic Ni was revealed by XRD after the reduction heat-treatments performed at temperatures higher than 500°C. The dependence of the phases content on reduction temperature is given in Fig.3. It should be noted that there is also some amount on the X-ray amorphous phase in the heat-treated powders. The content of spinel decreases and of nickel increases with the rise in temperature. Alumina crystals appear at temperatures of 900°C and above, their content increases with an increase of temperature.

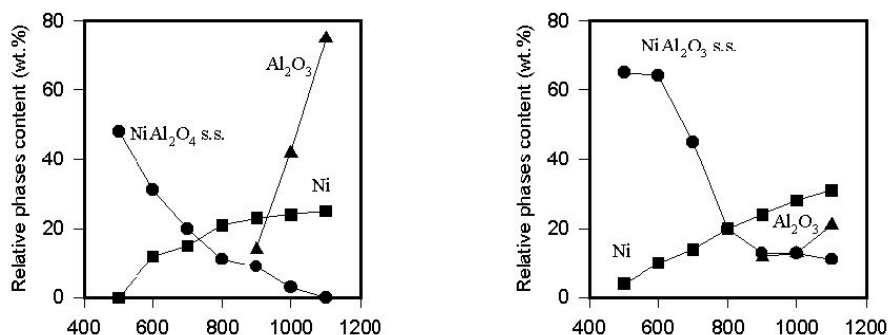


Fig.3. Relative phases content in powders vs. reduction temperature:  
a – composition 1, b - composition 2.

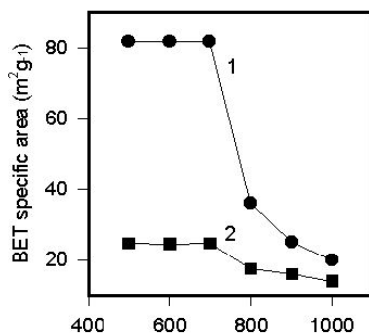


Fig.4. Effect of reduction temperature on specific area of the powders of series 1 and 2.

The specific surface area of the series 1 powders was drastically reduced from ca. 81 to 30  $\text{m}^2\text{g}^{-1}$  in the narrow range of temperature from 700 to 800°C (Fig.4), i.e. in the range where nickel and spinel contents are about the same. It can therefore be supposed that the high nickel content in respect to the oxides results in the enhanced agglomeration, this being because the interfacial Ni/Ni energy is lower than that for Ni/oxide interfaces [10]. This difference explains the driving force towards nickel agglomeration.

## Sintered materials

The sintering of the powders containing no sintering additions of titania and MnO at 1520°C in a vacuum results in further development of the phase composition, particularly in an increase of alpha-alumina content. The trends are shown in Fig.5 with dependence on the reduction of temperature. Residual porosity in sintered bodies was in the range 13.9 to 27.7%, measured by a water-replacement method. The pores are located at grain boundaries. The microstructure features were dependent on the reduction of temperature and on the phase composition of the powders. Generally, the deformed ceramic-metal agglomerates were observed microscopically. Within the agglomerates, fine nickel dispersoids were found whose diameter is substantially less than 1  $\mu\text{m}$ . Larger nickel particles as well as large pores were located at the agglomerates' junctions.

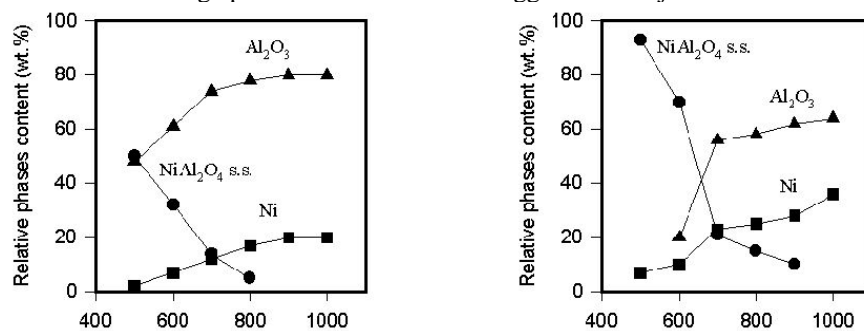


Fig.5. Relative phases content in sintered at 1500°C cermets vs. reduction temperature: a - composition 1, b - composition 2

Both the  $\text{TiO}_2$  and MnO additions lead to a decrease in porosity down to about 1-1.5% and to the coarsening of the microstructure. However, both the strength and fracture toughness of the materials sintered with the additives were low, about 350 MPa and 5.1  $\text{MPa}\cdot\text{m}^{1/2}$ , respectively. To improve the mechanical properties, experiments were performed with hot uniaxial pressing at a temperature of 1410°C. The results for compositions 1 and 2 containing and not containing the  $\text{TiO}_2$  sintering additive are given in Table 1. The properties of alumina ceramics, which have been fabricated at the same conditions, are given in the table for comparison.

Tab.1. Mechanical properties of hot-pressed at 1410°C cermets.

$\text{Al}_2\text{O}_3/\text{NiO}$	additive	Porosity [%]	Vickers hardness [GPa]	Bending strength [MPa]	Fracture toughness [ $\text{MPa}\cdot\text{m}^{1/2}$ ]
70/30	No	0.7	17.6	500	3.7
70/30	$\text{TiO}_2$ 2 wt. %	0.2	15.5	430	3.3
50/50	No	0.6	9.8	610	3.6
50/50	$\text{TiO}_2$ 2 wt. %	0.4	10.2	370	6.0
100/0	$\text{TiO}_2$ 2 wt. %	0.3	19.0	290	3.2

It follows from the data, that both the strength and fracture toughness for cermets exceed those for alumina ceramics containing no nickel phase. The effect is enhanced with an increase of nickel content. The requirements for the composition seems to be dependent

on the purpose, e.g. the highest strength value was obtained for the specimens containing no sintering additive and having relatively small grain size, whereas the highest fracture toughness was revealed for titania-containing materials of relatively coarse microstructure, the latter being a well-known phenomenon for ceramics exhibiting R-curve crack-growth behavior [14]. Obviously, further study is necessary to be performed, to find the conditions for lowering the grain size and improving the strength, as well as to evaluate the magnetic properties of the materials under development.

## CONCLUSION

Ultrafine Ni-nAl<sub>2</sub>O<sub>3</sub>-mNiO powders were synthesized by a heterophase interaction method followed by calcining in the air and reduction by H<sub>2</sub> gas. Trends in phase composition and in specific area of the powders were revealed in dependence on the processing route, and the influence of TiO<sub>2</sub> and MnO sintering additives on the microstructure and properties were studied as well. It was particularly shown that the specific area of the powder depends strongly upon its composition and heat-treatment schedule. High nickel content, in respect to oxides, results in an enhanced agglomeration. Sintered cermets exhibit potentially high fracture resistance, in excess of 6 MPa.m<sup>1/2</sup>, and their strength can principally be enhanced by reducing the grain size to a range in tens up to one hundred nanometers.

## Acknowledgement

The study is supported by the RAS programme “Nanomaterials and Supramolecular Structures” and by the bilateral agreement between the Russian and Slovakian Academies of Sciences and by the Slovak Grant Agency for Science under grants No: 2/1166/21 and 2/7011/20

## REFERENCES

- [1] Krstic, VV., Nicholson, PS., Hoagland, RG.: J. Am. Ceram. Soc., vol. 64, 1981, p. 499
- [2] Sekino, T., Nakajima, T., Ueda, S., Niihara, K.: J. Am. Ceram. Soc., vol. 80, 1997, p. 1139
- [3] Tuan, WH., Brook, RJ.: J. Europ. Ceram. Soc., vol. 10, 1992, p. 95
- [4] Barinov, SM., Fateeva, LV., Shevchenko, VYa., Yurashev, SV., Shvorneva, LI.: Mater. Res. Bull., vol. 33, 1998, p. 349
- [5] Sung, X., Yeomans, J.: J. Am. Ceram. Soc., vol. 79, 1996, p. 2705
- [6] Chen, RZ., Tuan, WH.: J. Europ. Ceram. Soc., vol. 19, 1999, p. 463
- [7] Trusty, PA., Yeomans, J.: J. Europ. Ceram. Soc., vol. 17, 1997, p. 495
- [8] Lopez-Esteban, S., Bartolome, JF., Moya, JS., Sagisaka, A., Matsumoto, K. In: Fractography of Advanced Ceramics. Ed. J. Dusza. TransTech Publ., Switzerland, 2002, p. 79
- [9] Roy, RA., Roy, R.: Mater. Res. Bull., vol. 19, 1984, p. 169
- [10] Grossmann, J., Sporn, D. In: Fourth Euro-Ceramics. Vol. 4. Basic Science. Ed. A. Belossi et al. Faenza Editrice S.p.A., Faenza, 1996, p. 21
- [11] Pierre, AC.: Amer. Ceram. Soc. Bull., vol. 70, 1991, p. 1281
- [12] Levin, BE., Tretjakov, YuD., Letuk, YuM. In: Physics and Chemistry Fundamentals of Preparation, Properties and Application of Ferrites. Moscow : Metallurgy, 1972, p. 128
- [13] Galakhov, FJa. In: Phase Diagrams for Refractory Oxide Systems. Vol. 5. Binary Systems. Leningrad : Science, 1985, p. 157
- [14] Barinov, SM., Shevchenko, VJa. In: Strength of engineering ceramics. Moscow : Science, 1996, p. 180